Journal of GeoSpace Science

ISSN-xxx-xxx
Open Access Biannual Research Journal publish by Institute of Space and Planetary Astrophysics

Journal home page: http://www.jogss.org/

Strong Gravitational Lensing by a Black Hole in Scalar-Tensor-Vector Modified Gravity (MOG)

Saqib Hussain, Azka Younas, Mubasher Jamil

School of Natural Sciences (SNS), National University of Sciences and Technology (NUST), Islamabad, Pakistan

ARTICLE INFO

Article history:
Received 8 September 2015
Received in revised form 12 September 2015
Accepted 15 September 2015
Available online 24 September 2015

Keywords: *Black hole; gravitational lensing; null-geodesics.*

ABSTRACT

We investigate the gravitational lensing scenario due to a black hole in modified gravity. We discuss here three special cases of modified gravity black hole: non-extreme, extreme and naked singularity. We present the detailed derivation for the bending angles of light by using the null geodesics as its traverses in the equatorial plane of the MOG black hole. We explore the energy conditions for the photons that when it will capture or escape from the black hole vicinity. We also investigate the characteristic of unstable circular orbit with reference to different parameters. Analysis of geodesics motion for photon is also discuss in this paper.

To Cite This Article: Saqib Hussain; Azka Younas and Mubasher Jamil., Strong Gravitational Lensing by a Black Hole in Scalar-Tensor-Vector Modified Gravity (MOG)., ***Jour. of GeoSpace Science, 1(1)***, *51-64, 2015*

INTRODUCTION

Since it was first published nearly a century ago, general relativity (GR) has earned its place as an incredibly successful and well verified theory of gravity (see e.g. (Will, 2006)). There are however, both theoretical and observational reasons to consider alternatives to, and extensions of, GR. Scalar-Tensor theories, which modify gravity by introducing new, non-minimally coupled scalar fields are an extensively studied alternative to GR. They are theoretically attractive because such light scalar fields are generically predicted in the low energy limit of string theory. For a scalar field to affect cosmological expansion, its mass must be of the order of the Hubble scale, $H_0 \times 10^{33} eV$. If it interacts with matter however, the presence of a light scalar field will result in a long-range fifth force and would thus be subject to tight constraints from laboratory and solar system tests of gravity (Will, 2006), (Bertotto et al., 2003) and (Williams et al., 2004).

The Scalar-Tensor-Vector-Gravity (STVG) (Moffat, 2006) based on completely relativistic gravity called modified gravity (MOG) leads to a gravity theory that can describe astrophysical and cosmological data. The STVG theory has an extra degree of freedom, a vector field (ϕ_μ) whose curl is a skew field that couples to matter. The gravitational field is described by a symmetric Einstein metric tensor. The classical theory allows the gravitational coupling constant (G) to vary as a scalar field with space and time. The effective mass (μ) of the phion field also varies with space and time as a scalar field. MOG theory has successfully explained the solar system observations (Moffat [5]), the rotation curves of galaxies (Moffat and Rahvar, 2013) and (Moffat and Toth, 2015), and the dynamics of galactic clusters (Moffat and Rahvar, 2014) and (Brownstein and Moffat, 2007), as well as

Corresponding Author: Mubasher Jamil, National University of Sciences and Technology (NUST), H-12, Islamabad, Pakistan.
E-mail: mjamil@sns.nust.edu.pk

describing the growth of structure, the matter power spectrum and the cosmic microwave background (CMB) acoustical power spectrum data (Moffat [10]).

Observations of high redshift supernovae indicate that the universe is expanding at an accelerating rate (Riess et al., 1998), (Perlmutter et al., 1999), and together with microwave background (Hinshaw et al., 2013) and (Ade at al., [14] and large scale structure (Abazajian et al., 2009) measurements, suggest that around 70 percent of the energy density of the universe comes in the form of 'dark energy'. Its energy density has a large negative pressure and is well modeled by a cosmological constant. The magnitude of cosmological constant is extremely small by particle physics standards, explaining its stability under quantum corrections is a challenge. Finding either a natural explanation for its measured value or an alternative to the constant, is a major motivation for developing and studying modified theories of gravity (see (Clifton et al., 2012) for a review of various approaches). Additionally, studying modified gravity theories allows us to better explore where GR has been tested rigorously and to constrain the low energy properties of quantum gravity theories.

The subject of black hole gravitational lensing has received growing attention since the discovery of supermassive black holes at the center of galaxies, in particular the one associated with SgrA* in the Milky Way. The light rays passing close to the photon sphere have a large deviation, and the deflection angle can be calculated by using the strong deflection limit (consisting in a logarithmic approximation) which was introduced some decades ago (Darwin and Roy, 1959) for the Schwarzschild spacetime. This method allows for the calculation of the positions, magnifications, and the time delays of the relativistic images. It was rediscovered several times (Luminet and Astron, 1979), then extended to the Reissner-Nordstrom metric (Eiroa et al., 2002), and to any spherically symmetric object with a photon sphere (Bozza, 2002). When the lens is a very compact object (e.g. a black hole) the weak field approximation is no longer valid. Strong field situation is recently studied in (Virbhadra, Ellis, 2002). They obtained the lens equation using an asymptotically flat background metric and analyzed the lensing by a Schwarzschild black hole in the center of the galaxy using numerical methods. Besides the primary and secondary images, they found that there exist two infinite sets of faint relativistic images. (Frittelli et al., 2000) found an exact lens equation without any reference to a background metric and they also compared their results with (Virbhadra, Ellis, 2002) for the Schwarzschild black hole case. (Bozza et al., 2001) analytical expressions for the positions and magnification of the relativistic images was obtained using the strong field limit approximation.

Within this context, black hole solution in Scalar-Tenor-Vector modified gravity with spherical symmetry was found in (Moffat, 2015). In Sec. II we introduce the basic equations for lensing (null geodesics) using the MOG black hole metric. In Sec. III we calculate the critical variable of circular orbits for photons. In Sec. IV we analyze the dynamics of photons in the surroundings of MOG black hole and also discuss the conditions with respect to energy of photon which correspond to different kind of motion of photon. In Sec. V we discuss the lens diagram and calculated the second order ordinary differential equation of path. In Sec. VI we compute the bending angle in the form of first kind of elliptical integral and do analysis the light deflection by changing the MOG parameter α. In Sec. VII we derive the formulae of radial and tangential magnification to compute the total amplification for the images.

2. Modified Gravity Black Hole Geometry

The MOG action with respect to field results takes the form [4]

$$S = S_G + S_\phi + S_S + S_M, \tag{1}$$

where

$$S_G = -\frac{1}{16\pi}\int \frac{1}{G}(R+2\Lambda)\sqrt{-g}\,d^4x, \tag{2}$$

$$S_\phi = -\int \omega\left[\frac{1}{4}B^{\mu\nu}B_{\mu\nu} - \frac{1}{2}\mu^2\phi^\mu\phi_\nu + V_\phi(\phi)\right]\sqrt{-g}\,d^4x, \tag{3}$$

$$S_S = \int \frac{1}{G}[\frac{1}{2}g^{\mu\nu}(\frac{\Delta_\mu G\Delta_\nu G}{G^2} + \frac{\Delta_\mu\mu\Delta_\nu\nu}{\mu^2}) - \frac{V_G(G)}{G^2} - \frac{V_\mu(\mu)}{\mu^2}]\sqrt{-g}\,d^4x. \tag{4}$$

For the metric $g_{\mu\nu}(x)$, we have a massive vector field $\phi_\mu(x)$, and two scalar fields $G(x)$ and $\mu(x)$ .Further, $V_\phi(\phi)$, $V_G(G)$ and $V_\mu(\mu)$ denote self-interaction potentials whereas ω is a dimensionless constant and λ is a cosmological constant. Moreover

$$B_{\mu\nu} = \partial_\mu\phi_\nu - \partial_\nu\phi_\mu. \tag{5}$$

The action for pressureless dust can be written as

$$S_M = \int\left[\rho\sqrt{u^\mu u_\nu} - \omega Q_5 u^\mu\phi_\mu\right]\sqrt{-g}\,d^4x, \tag{6}$$

here ρ is the matter density and $Q_5 = k\rho$ is the source charge of fifth force which is related to density of mass where k called constant,

$$k = \pm\sqrt{\alpha G_N}, \qquad Q = \pm\sqrt{\alpha G_N}M. \tag{7}$$

For the gravitational charge $Q > 0$ so we choose positive value. We study the STVG field equation for the metric tensor $g_{\mu\nu}$ [4]

$$R_{\mu\nu} = -8\pi G T_{\phi\mu\nu}, \tag{8}$$

where G is called coupling constant, the matter energy-momentum tensor $T_{M\mu\nu} = 0$. We have the energy-momentum tensor $T_{\phi\mu\nu}$ for the ϕ_μ vector field is [1]

$$T_{\phi\mu\nu} = -\frac{1}{4\pi}\left(B_\mu^\alpha B_{\nu\alpha} - \frac{1}{4}g_{\mu\nu}B^{\alpha\beta}B_{\alpha\beta}\right). \tag{9}$$

MOG black hole (Moffat, 2015) has a static spherically symmetric solution with mass M . Its geometry is expressed in terms of element with spherical coordinates (t,r,θ,ϕ) as

[1] By the definition [4] for the energy-momentum tensor $T_{\phi\mu\nu}$ the potential $V(\phi)$ is zero.

$$ds^2 = f(r)c^2dt^2 - f(r)^{-1}dr^2 - r^2d\theta^2 - r^2\mathrm{Sin}^2\theta d\phi^2, \tag{10}$$

Where

$$f(r) = 1 - \frac{2GM}{c^2r} + \frac{\alpha G_N GM^2}{r^2}. \tag{11}$$

Here $G = G_N(1+\alpha)$, G_N is Newton's constant, $\alpha = \frac{G}{G_N} - 1$ is a MOG black hole parameter and M is the mass of the MOG black hole. The black hole has two horizons like RN black hole and it will reduce to Schwarzschild black hole for $\alpha = 0$.

In above metric "curvature singularity" arises at $r = 0$, where $f(r) \to \infty$ and "coordinate singularity" arises when $f(r) = 0$, which gives the two horizons

$$r_{\pm} = G_N(1+\alpha)M(1 \pm \sqrt{1 - \frac{\alpha}{1+\alpha}}), \tag{12}$$

Here $r_+ = r_H$ gives the event or outer horizon while r_- is the inner horizon.

$$r_H = G_N(1+\alpha)(1+\sqrt{1-\frac{\alpha}{1+\alpha}})M, \tag{13}$$

When $\alpha = 0$ and $G = G_N$ then MOG black hole event horizon (r_H) reduces into Schwarzschild black hole (SBH) event horizon $(r_H^S = 2GM)$. In the case of photon, we use λ as an affine parameter. Our geometry is spherically symmetric and we want particle to be restricted in the equatorial plane $(\theta = \frac{\pi}{2})$, so according to above conditions, the Lagrangian for a photon traveling in MOG spacetime is given by

$$\mathrm{L} = f(r)\dot{t}^2 - f(r)^{-1}\dot{r}^2 - r^2\dot{\phi}^2,$$

$$f(r) = 1 - \frac{2G_N(1+\alpha)M}{r} + \frac{\alpha G_N^2(1+\alpha)M^2}{r^2} \tag{14}$$

The Euler-Lagrange equations for null geodesics, gives

$$\dot{t} \equiv \frac{dt}{d\lambda} = \frac{E}{f(r)}, \tag{15}$$

$$\dot{\phi} \equiv \frac{d\phi}{d\lambda} = \frac{L}{r^2}. \tag{16}$$

In Eqs. (15) and (16), E is the energy per unit mass and L is the angular momentum per unit mass. To calculate the equation of motion for photon (radial equation) for MOG spacetime (10) substituting Eqs. (15) and (16) in the null condition of the 4-velocity $g_{\mu\nu}\dot{x}^\mu\dot{x}^\nu = 0$ [2] where $\dot{x}^\mu = \frac{dx^\mu}{d\lambda}$ is the 4-velocity.

[2] Greek letters $(\mu,\nu = 0,1,2,3)$ for spacetime indices, where 0 correspond to time coordinate t and $1,2,3$ correspond to r, θ, ϕ

$$\dot{r} = L\sqrt{\frac{1}{b^2} - \frac{f(r)}{r^2}}, \quad where \quad b = |\frac{L}{E}|. \tag{17}$$

Here b is the impact parameter for a photon of finite rest mass (Thorne et al., 1973). From Eq. (17), obtain the effective potential for photons which is given by

$$\mathrm{U}_{\mathrm{eff}} = \frac{L^2}{r^2} f(r) = \frac{L^2}{r^2} - \frac{2G_N(1+\alpha)ML^2}{r^3} + \frac{\alpha G_N^2(1+\alpha)M^2L^2}{r^4}. \tag{18}$$

First term corresponds to the centrifugal potential. The second term represent the relativistic correction due to general relativity. The third term due to the fact that MOG black hole geometry depends a parameter α. This potential has a maximum which means that photon has unstable circular orbit and does not have any stable orbit around MOG black hole. In Eq. (18), when $\alpha = 0$ it reduces in SBH effective potential $(\mathrm{U}_{\mathrm{eff}}^{S})$

$$\mathrm{U}_{\mathrm{eff}}^{S} = \frac{L^2}{r^2}(1 - \frac{2GM}{r}). \tag{19}$$

3. Critical Variables of Circular Orbits for MOG Black Hole

For the circular orbits, we take the critical parameters as $(r_o = r_{ps})$ and $(b_S = b_{SC})$.

We take the Eq. (18) to calculate the critical value of closest approach (r_o). Apply the circular orbit condition $\frac{dU_{\mathrm{eff}}}{dr}|_{r=r_o} = 0$ on it which gives us

$$r_{o_\pm} = \frac{3}{2}GM\left(1 \pm \sqrt{1 - \frac{8}{9}\frac{G_N}{G}\alpha}\right) \tag{20}$$

Here r_{o_-} is greater than the outer horizon r_+ while r_{o_+} lies between inner and outer horizon $(r_- < r_{o_+} < r_+)$. The region of interest is between the horizons that is r_{o_+}. Therefore, the radius of unstable circular orbit for photon (photon sphere) is

$$r_{ps} = \frac{3}{2}G_N(1+\alpha)M(1 + \sqrt{1 - \frac{8}{9}\frac{\alpha}{(1+\alpha)}}). \tag{21}$$

Further, to calculate the value of the impact parameter b, apply the second condition of circular orbit for the closest approach $\frac{dr}{d\lambda}|_{r=r_o} = 0$ in Eq. (18), we obtain

$$b(r_O) = \frac{r_O}{\sqrt{1 - \frac{2G_N(1+\alpha)M}{r_O} + \frac{\alpha G_N^2(1+\alpha)M^2}{r_o^2}}}, \tag{22}$$

here we replace r_o with r_{ps}, which gives us the critical value of impact parameter for MOG black hole. Further, when $\alpha = 0$ it reduces in SBH impact parameter $b_{SC} = 3\sqrt{3}GM$.

4. Dynamics of Photon

First we will discuss the effective potential of MOGBH with respect to a photon. Effective potential is given by (18) and we can rewrite it as,

$$\dot{r}^2 + \mathrm{U}_{\mathrm{eff}} = E_n^2. \tag{23}$$

To study the behaviour of photon against r, we have plotted $\mathrm{U}_{\mathrm{eff}}$ for different value α in Fig. 1.

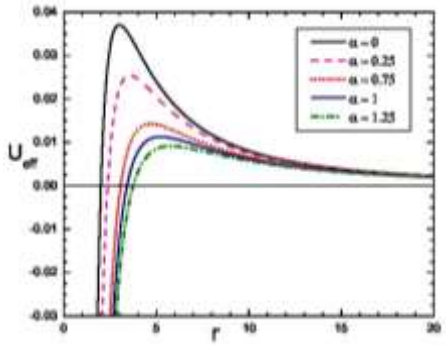

Fig. 1: Effective potential $\mathrm{U}_{\mathrm{eff}}^{e}$ is shown as a function of distance r for a different values of α. Upper curve for Schwarzschild's effective potential is taken as a reference $(\alpha = 0)$ while the other curves for regular MOG black hole for $\alpha > 0$.

Fig. 1 shows that from effective potential, we studied the behavior of photons surroundings the MOG black hole. Effective potential depends on the MOG parameter α. We take $M = 1$ and $G_N = 1$. We observed that as we increase the value of α there is no change in the photon orbits means there is no minima so there is no stable circular orbit for photon only unstable orbit exists.

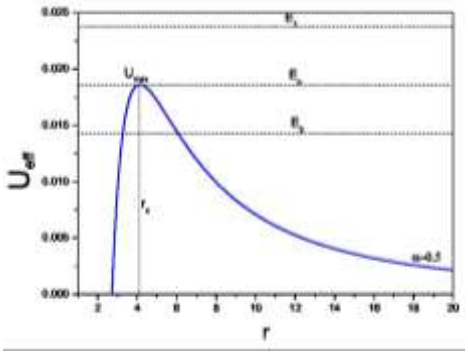

Fig. 2: Here we have Plotted the effective potential as a function of r for $G_N = 1$.

The relation between energy and effective potential is given by Eq. (23) and the motion of photon depends on the energy levels. In Fig. 2, the effective potential is plotted for single value of $\alpha = 0.5$ and there are three energy levels, E_1, E_C and E_3.

Case 1: $E_n = E_C$

If the energy of photon is equal to E_c then we have from Eq. (23), $E_n^2 - \mathrm{U}_{\mathrm{eff}} = 0$ and $\dot{r} = 0$. This condition corresponds to circular orbit of photon.

Due to the nature of the potential at r = rc, these are unstable orbits.

Case 2: $E_n = E_3$

Here, $E_n^2 - U_{eff} \geq 0$ in two regions as is clear from Fig. 2. If the photons start the motion at $r > r_c$, or its energy is less then $E_n < E_c$, it will move back to large values of r.

If the photons start the motion at $r < r_c$, then the photons will fall into the singularity.

Case 3: $E_n = E_3$

For $E_n^2 > E_c$, or $E_n^2 - U_{eff} > 0$ and $\dot{r} > 0$ and the photons coming from large r values will cross the horizon and will fall into the singularity.

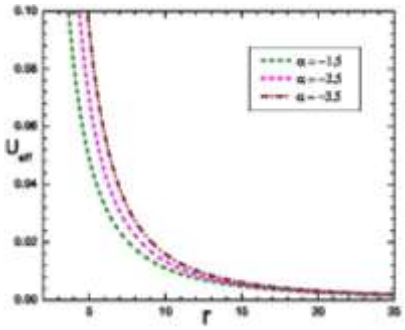

Fig. 3: Effective potential U_{eff} is shown as a function of distance r for $\alpha < -1$ (naked singularity).

Fig. 3: shows that the effective potential is a monotonically decreasing function in the interior region of MOG black hole. So it does not have any extremum, however in the interior region there is no photon sphere present. At the singularity effective potential blows up which implies that light rays may not reach in the interior region of MOG black hole.

4.1. The Time Period

The time period (T_λ) for an unstable circular orbit of photon can be calculated by Eq. (16), as

$$T_\lambda = \frac{2\pi r_c^2}{L}. \tag{24}$$

For the Schwarzschild BH it is given as $$T_\lambda = \frac{2\pi(3M)^2}{L}. \tag{25}$$

Since the radius r_c is smaller for the Schwarzschild black hole, T_λ is smaller for the SBH. We have plotted the Eq. (21) for the circular orbit r_c of photon as a function of α. It can be seen from the Fig. 4 that the radius of the orbit r_c getting larger for large value of α. Hence, for large value of α there is a positive shift in the orbit from the horizon. For $\alpha > 1$, the orbit might shift closer to horizon as $\alpha > 1$, is corresponding to naked singularity.

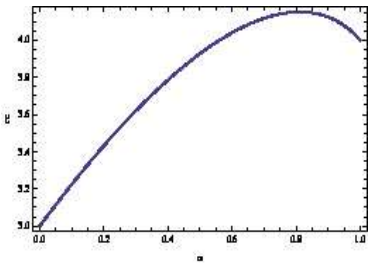

Fig. 4: Here we have plotted the radius of circular orbit for photon r_c against α.

4.2. Geodesic Motion of Photon

For a particle coming toward the MOG black hole and the geodesics equation could be obtained by using Eqs. (15) and (17) we have:

$$\frac{dt}{dr} = \pm \frac{E}{f(r)\sqrt{E^2 - (\frac{L^2}{r^2}) f(r)}}, \tag{26}$$

Here positive sign is for the particle going away from the BH, and negative sign gives the path of an ingoing particle. Let us consider the particle which is coming from infinity, initially at rest, approaches the BH, we plot the geodesics in (r,t) coordinates, see Fig. 5.

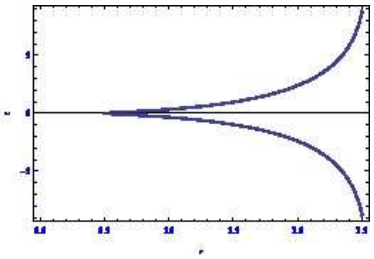

Fig. 5: In this figure we have plotted t against r for $\alpha = 0.5$. Geodesics of an ingoing particle coming from infinity initially at rest and going back to infinity.

5. Equation of Path and Conversion the Distance in term of Schwarzschild Radius

For the equation of path for photons, divide Eq. (17) with Eq. (16), gives the second order ordinary differential equation.

$$(\frac{dr}{d\phi})^2 = r^2[\frac{r^2}{b^2} - (1 - \frac{2G_N(1+\alpha)M}{r} + \frac{\alpha G_N^2(1+\alpha)M^2}{r^2})]. \tag{27}$$

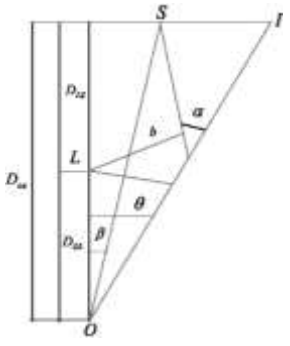

Fig. 6: The lens diagram. The positions of observer (O), source (S), lens (L) and image (I) are shown in the figure. The observer-lens, lens-source and observer-source distances are represented by D_{OL}, D_{LS} and D_{OS} respectively.

Our gravitational lensing phenomenon can be represented as it is shown in Fig. (6). When we observe this phenomenon, at the closest approach $r_o \rightarrow r_{ps}$ (region of photon sphere where the bending of light occurs) here the bending angle $\hat{\alpha} > 2\pi$, whereby the light can turn around the MOG black hole severals times before reaching the observer. We found two finite sets of images, one produced by clockwise winding around MOG black hole for $\hat{\alpha} > 0$ and the other one counter-clockwise winding for $\hat{\alpha} < 0$. These images are called relativistic images. When $\hat{\alpha} < \frac{3\pi}{2}$, the light will deflect without turning around MOG black hole and reaches the observer then primary and secondary images are observed. These images are located the same side or opposite side of the source. The lens equation can be expressed as (Virbhadra, Ellis, 2002)

$$\tan\beta = \tan\theta - \frac{D_{LS}}{D_{OS}}[\tan(\hat{\alpha} - \theta) + \tan\theta], \tag{28}$$

$$b(r_o) = D_{OL}\sin\theta. \tag{29}$$

Angular positions of source and images are represented by β and θ respectively while the deflection angle due to black hole is denoted by $\hat{\alpha}$ as it is showed in the Fig. (6).

To make the quantities dimensionless, converting the distances in terms of the Schwarzschild BH's radius i.e.

$$X = \frac{r}{2M}, \quad X_o = \frac{r_o}{2M}, \quad b(r_o) = 2Mb(X_0).$$

$$d_{ol} = \frac{D_{OL}}{2M}, \quad d_{os} = \frac{D_{OS}}{2M}, \quad d_{ls} = \frac{D_{LS}}{2M}. \tag{30}$$

By using these definition, we convert the Eqs. (13), (21) and (22) in term of x_o.

$$X_H = \frac{G_N}{2}(1+\alpha)(1+\sqrt{1-\frac{\alpha}{1+\alpha}}), \tag{31}$$

$$X_{ps} = \frac{3}{4}G_N(1+\alpha)(1+\sqrt{1-\frac{8}{9}\frac{\alpha}{(1+\alpha)}}), \tag{32}$$

$$b_{sc}(X_o) = \frac{X_o}{\sqrt{1-\frac{G_N(1+\alpha)}{X_o}+\frac{\alpha G_N^2(1+\alpha)}{4X_o^2}}}, \tag{33}$$

Further, also convert Eq. (27) in term of distance and then substitute the Eq. (33) in it, yields

$$(\frac{dX}{d\phi})^2 = X^2[\frac{X^2}{X_o^2}(1-\frac{G_N(1+\alpha)}{X_o}+\frac{\alpha G_N^2(1+\alpha)}{4X_o^2})-(1-\frac{G_N(1+\alpha)}{X}+\frac{\alpha G_N^2(1+\alpha)}{4X^2})], \tag{34}$$

it can also be write as S

$$\frac{d\phi}{dX}=\pm\frac{1}{X\sqrt{(\frac{X}{X_o})^2(1-\frac{G_N(1+\alpha)}{X_o}+\frac{\alpha G_N^2(1+\alpha)}{4X_o^2})-(1-\frac{G_N(1+\alpha)}{X}+\frac{\alpha G_N^2(1+\alpha)}{4X^2})}}. \tag{35}$$

6. Bending Angle and Elliptic Variable for MODBH

Suppose that a light ray coming from infinity $(-\infty)$ reaches the MOG black hole at x_o and finally it approaches again to infinity $(+\infty)$ (observer). Due to this a change, the angular coordinate ϕ is twice from infinity to x_o. The light ray deflects from a straight line path at the difference of π which results in bending angle. We use the bending angle formula (Weinberg, 1972):

$$\alpha=2\int_{X_o}^{\infty}\frac{d\phi}{dX}dX-\pi, \tag{36}$$

In Eq. (35), positive sign $(+)$ shows that the angle ϕ changes more than π, that is the photon trajectory is bent toward the MOG black hole and for negative sign $(-)$ photon trajectory bent away from the MOG black hole. We substitute Eq. (35) in (36) which gives the bending angle for MOG black hole as

$$\hat{\alpha}(X_o)=2\int_{X_o}^{\infty}\frac{dX}{X\sqrt{(\frac{X}{X_o})^2(1-\frac{G_N(1+\alpha)}{X_o}+\frac{\alpha G_N^2(1+\alpha)}{4X_o^2})-(1-\frac{G_N(1+\alpha)}{X}+\frac{\alpha G_N^2(1+\alpha)}{4X^2})}}-\pi, \tag{37}$$

it can be also be rewritten as

$$\hat{\alpha}(X_o)=\frac{4X_o}{\sqrt{1-\frac{G_N(1+\alpha)}{X_o}+\frac{\alpha G_N^2(1+\alpha)}{4X_o^2}}}\int_{X_o}^{\infty}\frac{dX}{\sqrt{P(X)}}-\pi, \tag{38}$$

where

$$P(X)=X^4+(-X^2+G_N(1+\alpha)X-\frac{\alpha G_N^2(1+\alpha)}{4})(\frac{X_o^2}{1-\frac{G_N(1+\alpha)}{X_o}+\frac{\alpha G_N^2(1+\alpha)}{4X_o^2}}), \tag{39}$$

Eq. (39) is a fourth degree polynomial in term of X whose roots depends on x_o and α, where $x_o > x_{ps}$ and the limits on the roots are $X_1 > X_2 > X_3 > X_4$. Further applying some limitation on α that are: , $\alpha > 0$, MoG black hole has two horizon (non-extreme) while $\alpha < -1$, MOG black hole has no horizon (naked singularity). Thus, the roots are

$$X_1=X_o, \tag{40}$$

$$X_2=\frac{1}{6L(R+M)}[2^{5/3}NX_o^2-2L(R+M)X_o+2\sqrt[3]{2}(R+M)^2], \tag{41}$$

$$X_3=\frac{1}{12L(R+M)}[2^{5/3}\left(1+i\sqrt{3}\right)NX_o^2-4L(R+M)X_o+2i\sqrt[3]{2}\left(\sqrt{3}+i\right)(R+M)^2], \tag{42}$$

$$X_4 = \frac{1}{12L(R+M)}[2^{5/3} i\left(\sqrt{3}+i\right) N X_O^2 - 4L(R+M)X_O - 2\sqrt[3]{2}\left(1+i\sqrt{3}\right)(R+M)^2], \tag{43}$$

Further, L, R, M and N are the part of the roots that depends on the G_N, X_o and α

$$L = \alpha(\alpha+1)G_N^2 - 4(\alpha+1)G_N X_O + 4X_O^2. \tag{44}$$

$$R = \sqrt[3]{33\alpha^2(\alpha+1)^3 G_N^5 X_O^4 - 5\alpha^3(\alpha+1)^3 G_N^6 X_O^3 + 96(2+3\alpha+\alpha^2)G_N^2 X_O^7 - 32X_O^9}$$

$$+\sqrt[3]{8(\alpha+1)^2(\alpha-14)G_N^3 X_O^6 - 48(\alpha+1)G_N X_O^8 - 6\alpha(\alpha+1)^2(11\alpha+4)G_N^4 X_O^5} \tag{45}$$

$$M = \sqrt[3]{3\sqrt{3}\sqrt{(\alpha^3((\alpha+1)^2 G_N^4 - 2\alpha^2(\alpha+1)^2 G_N^3 X_O)(\alpha+1)G_N^2 L^3 X_O^6)}}$$

$$+\sqrt[3]{3\sqrt{3}\sqrt{(\alpha\left(\alpha^2+6\alpha+5\right)G_N^2 X_O^3 + 4X_O^4)(-(\alpha+1)^2 G_N^2 L^3 X_O^6)}}$$

$$+\sqrt[3]{3\sqrt{3}\sqrt{12\alpha G_N^3 L^3 X_O^1 0}}. \tag{46}$$

$$N = 8\alpha(\alpha+1)^2 G_N^3 X_O - \alpha^2(\alpha+1)^2 G_N^4 - 2(9\alpha^2+17\alpha+8)G_N^2 X_O^2 + 8(\alpha+1)G_N X_O^3 + 8X_O^4. \tag{47}$$

Now use these roots in Eq. (38) and write it in terms of first elliptic integral as

$$\hat{\alpha}(X_O) = G(X_O)F(\phi_O, \lambda) - \pi, \tag{48}$$

where

$$G(X_O) = \frac{4X_O}{\sqrt{1 - \frac{G_N(1+\alpha)}{X_O} + \frac{\alpha G_N^2(1+\alpha)}{4X_O^2}}} \frac{1}{\sqrt{(X_1 - X_3)(X_2 - X_4)}}, \tag{49}$$

and

$$F(\phi_O, \lambda) = \int_0^{\phi_O} \frac{1}{\sqrt{1 - \lambda \mathrm{Sin}^2\phi}} d\phi. \tag{50}$$

Here the integral can be recognized as first kind of elliptic integral [3] with arguments

$$\phi_O = \mathrm{Sin}^{-1}\sqrt{\frac{X_2 - X_4}{X_1 - X_4}}. \tag{51}$$

$$\lambda = \frac{(X_1 - X_4)(X_2 - X_3)}{(X_1 - X_3)(X_2 - X_4)}. \tag{52}$$

According to Figs. (7) and (8) : we observed that for large distance from MOG black hole the deflection of light reduces. For MOG black hole the deflection angle $\hat{\alpha}$ depends on MOG parameter

[3] The integral involving a rational function which contains square roots of cubic or quartic polynomials. Generally, here a definite quartic integral that has a build in command in Mathematica as: $F[\phi, m]$ having range $-\frac{\pi}{2} < \phi < \frac{\pi}{2}$ by $F(\phi \mid m) = \int_0^{\infty} \frac{1}{\sqrt{1 - m\sin^2\theta}} d\theta$

α and when we increase its value, deflection of light toward MOG black hole becomes large. Thus, bending angle $\hat{\alpha}$ in case of MOG black hole is greater than SBH. On the other side for the negative value of α (case of naked singularity with no horizons) bending angle is still positive because the sign of ϕ in the equations of motion is determined by the incident ray in the asymptotic region since in this case light deflection is smaller so the bending angle is smaller than SBH.

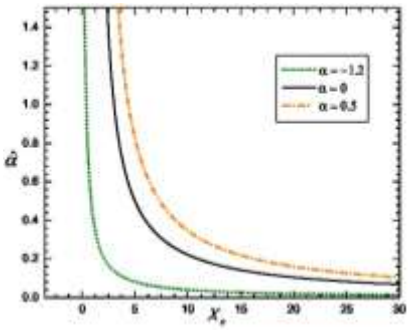

Fig. 7: Strong bending angle $(\hat{\alpha})$ is a function of closest distance X_o. All the curves shows the behavior of bending angle due to deflection of light surroundings in MOG black hole. upper cure for $\alpha = 0.5$ two horizons case. At $\alpha = 0$ middle curve for SBH bending angle that is taken as reference and bottom curve for naked singularity where $\alpha = -1.2$.

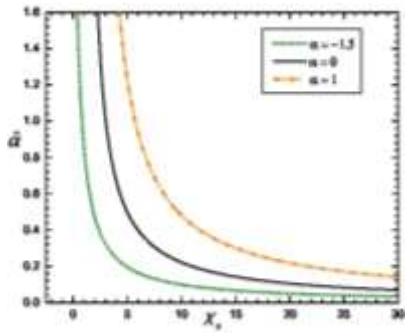

Fig. 8: Strong bending angle $(\hat{\alpha})$ is a function of closest distance X_o. For $\alpha = 1$ case of two horizons . At $\alpha = 0$ middle curve for SBH bending angle that is taken as reference and bottom curve for naked singularity where $\alpha = -1.5$.

In addition for the higher value of α both cases are much more pronounced. Plots for other values of α look similar to this, and in the limit $\alpha = 0$, all three curves merge as expected.

One important feature is the bending angle suppression for the negative value of α compared to SBH case. Light rays are bent more downstream with the positive value of α while the upstream motion of light rays gives smaller bending angles with negative values of α. In MOG black hole for both positive and negative value of α like SBH case, relativistic images are formed with the multiple loops when the bending angle exceeds 2π. As seen by an observer, the difference between both cases these images would be counterbalanced to different amount on both sides of MOG black hole.

7. Magnification for MOG Lens

When the source position is fixed, we want to calculate the images position and magnifications.

All values that is related to θ satisfied the lens Eq. (28) for fixed value of source position β tells us the location of the images.

For this, we write the deflection angle $\hat{\alpha}(X_o)$ in terms of the source position $\hat{\alpha}(\theta)$. According to the Liouville's theorem implies that surface brightness is preserved. Thus, the ratio of the flux of the image to the flux of the source is the ratio of the solid angle subtended by the image to that of the source at the location of the observer. Generally, for a circular symmetric lens, the total magnification for the images is given by (Virbhadra, Ellis, 2002).

$$\mu = |\frac{\sin\beta}{\sin\theta}\frac{d\beta}{d\theta}|^{-1}. \tag{53}$$

Eq. (53) gives the tangential and radial magnifications for images are respectively defined as

$$\mu_t \equiv (\frac{\sin\beta}{\sin\theta})^{-1} \quad , \quad \mu_r \equiv (\frac{d\beta}{d\theta})^{-1}. \tag{54}$$

The magnification sign of an image gives the parity of the image. The tangential and radial critical curves occurs in the lens plane at the singularities of the tangential and radial magnifications respectively, in the source plane radial and tangential caustics occur. By differentiating both sides of Eq. (28) radial magnification can be written as

$$\frac{d\beta}{d\theta} = (\frac{\cos\beta}{\cos\theta})^2[1-\frac{d_{ls}}{d_{os}}(1+(\frac{\cos\theta}{\cos(\alpha-\theta)})^2(\frac{d\alpha}{d\theta}-1))], \tag{55}$$

where $\frac{d\alpha}{d\theta} = \frac{d\alpha}{dX_O}\frac{dX_O}{d\theta}$. By taking derivative with respect to X_o of Eq. (37), we obtain

$$\frac{d\alpha}{dX_O} = \int_{X_o}^{\infty} \frac{X(\alpha(\alpha+1)G_N^2 + X_o(2X_o - 3(\alpha+1)G_N))}{X_o^5\left(\frac{X^2\left(\alpha(\alpha+1)G_N^2 + 4X_o(X_o-(\alpha+1)G_N)\right)}{4X_o^4} - \frac{\alpha(\alpha+1)G_N^2}{4X^2} + \frac{(\alpha+1)G_N}{X} - 1\right)^{3/2}} dX. \tag{56}$$

Finally, by differentiating Eq. (33) with respect to θ on both sides and doing some simplifications we get

$$\frac{dX_O}{d\theta} = \frac{X_o\left(1-\frac{G_N(1+\alpha)}{X_o}+\frac{\alpha G_N^2(1+\alpha)}{4X_o^2}\right)^{\frac{3}{2}}\sqrt{1-\left(\frac{X_o}{d_{ol}}\right)^2\left(1-\frac{G_N(1+\alpha)}{X_o}+\frac{\alpha G_N^2(1+\alpha)}{4X_o^2}\right)^{-1}}}{\frac{1}{2d_{ol}}(2X_o - G_N(1+\alpha))}. \tag{57}$$

Conclusion

We have studied the phenomena of strong gravitational lensing where the lens is the MOG black hole. We have studied the equation of path for photons and null geodesics in detail. Behavior of light in the surroundings of MOG black hole is discussed by calculating the deflection angle. There is a parameter α which differentiate the MOG black hole solution from other solutions. Hence we focus on that bending angle, photon sphere and trajectories of photons would have changed due to this parameter. We found that for each value of α photons have only one unstable circular orbits and no such orbits exist for naked singularity. We have explored two different cases of lensing: (1). regular MOG black hole where $\alpha > 0$, (2). naked singularity $\alpha < -1$. In all cases behavior of bending angle is similar.

It is observed that bending angle decreases as the distance x_o from MOG black hole increases. We found that large value of α correspond to greater deflection opposite to RN- black hole lensing.

References

[1] Will C. M., 2006, Rev. Rel. 9, 3. (gr-qc/0510072).
[2] Bertotti B., Iess L., and Tortora P., 2003, Nature 425 (Sept., 2003).
[3] Williams J. G., Turyshev S. G. and Boggs D. H., 2004, Phys. Rev. Lett., 93, 261101. (gr-qc/0411113).
[4] Moffat J. W., 2006, JCAP, 0603, 004. (arXiv:gr-qc/0506021).
[5] Moffat J. W., arXiv:1410.2464 (gr-qc).
[6] Moffat J. W. and Rahvar S., 2013, MNRAS, 436, 1439. (arXiv:1306.6383 (astro-ph.GA)).
[7] Moffat J. W. and Toth V. T., 2015, Phys. Rev., D91, 043004 (2015). (arXiv:1411.6701 (astro-ph.GA)).
[8] Moffat J. W. and Rahvar S., 2014, MNRAS, 441, 3724. (arXiv:1309.5077 (astro-ph.CO).
[9] Brownstein J. R. and Moffat J. W., 2007, MNRAS, 382, 29. (arXiv:0702146 (astro-ph).
[10] Moffat J. W., arXiv/1409.0853 (astro-ph.CO).
[11] Riess A. G., et al., (Supernova Search Team Collaboration), 1998, J. 116, 1009. (astro-ph/9805201).
[12] Perlmutter S., et al. (Supernova Cosmology Project Collaboration), 1999, Astrophys. J. 517, 565 (astro-ph/9812133).
[13] Hinshaw G., et al. (WMAP Collaboration), 2013, Astrophys. J. Suppl.208 (19). (arXiv:1212.5226 (astro-ph.CO)).
[14] Ade P. A. R., et al. (Planck Collaboration), arXiv:1303.5076. (astro-ph.CO).
[15] Abazajian K. N., et al., (SDSS Collaboration), 2009, Astrophys. J. Suppl. 182, 543. (arXiv:0812.0649 (astro-ph)).
[16] Clifton T., Ferreira P. G., Padilla A. and Skordis C., 2012, Phys. Rept. 513. (arXiv:1106.2476 (astro-ph.CO)).
[17] Darwin C., 1959, Proc. Roy. Soc London A 249, 180.
[18] (a) Luminet J. P., Astron, 1979, Astrophys. 75, 228.
(b) Ohanian, 1987, Am. J. Phys., 55, 428.
(c) R.J. Nemiroff R. J., 1993, Am. J. Phys., 61, 619.
(d) Bozza V., Capozziello S., Iovane G., and Scarpetta G., 2001, Gen. Relativ. Gravit., 33, 1535.
[19] (a) Eiroa E. F., Romero G. E., and Torres D. F., 2002, Phys. Rev. D 66, 024010
(b) Eiroa E. F. and D.F. Torres D. F., 2004, Phys. Rev. D 69, 063004.
[20] Bozza V., 2002, Phys. Rev. D 66, 103001.
[21] Virbhadra K. S., Ellis G. F. R., 2000, Phys. Rev. D 62, 084003. (arXiv:astro-ph/9904193).
[22] Frittelli S., Kling T. P., Newman E. T., 2000, Phys. Rev. D 61, 064021.
[23] Bozza V., Capozzielo S., Iovane G., Scarpetta G., 2001, Gen. Rel. Grav., 33, 1535. (arXiv:gr-qc/0102068).
[24] Moffat J. W., 2015, arXiv:1412.5424v3 (gr-qc).
[25] Thorne K. S., Misner C. W. and J. A. Wheeler J. A., 1973, Gravitation.
[26] Weinberg S., 1972, Gravitation and Cosmology, Principles and Applications of the General Theory of Relativity.